



**HAL**  
open science

## Direct measurement of evapotranspiration from a forest using a superconducting gravimeter

Michel van Camp, Olivier de Viron, Gwendoline Pajot-Métivier, Fabien Casenave, Arnaud Watlet, Alain Dassargues, Marnik Vanclooster

### ► To cite this version:

Michel van Camp, Olivier de Viron, Gwendoline Pajot-Métivier, Fabien Casenave, Arnaud Watlet, et al.. Direct measurement of evapotranspiration from a forest using a superconducting gravimeter. *Geophysical Research Letters*, 2016, 10.1002/2016GL070534 . hal-01443355

**HAL Id: hal-01443355**

**<https://hal.science/hal-01443355>**

Submitted on 23 Jan 2017

**HAL** is a multi-disciplinary open access archive for the deposit and dissemination of scientific research documents, whether they are published or not. The documents may come from teaching and research institutions in France or abroad, or from public or private research centers.

L'archive ouverte pluridisciplinaire **HAL**, est destinée au dépôt et à la diffusion de documents scientifiques de niveau recherche, publiés ou non, émanant des établissements d'enseignement et de recherche français ou étrangers, des laboratoires publics ou privés.

See discussions, stats, and author profiles for this publication at: <https://www.researchgate.net/publication/308070868>

# Direct measurement of evapotranspiration from a forest using a superconducting gravimeter

Article in *Geophysical Research Letters* · September 2016

DOI: 10.1002/2016GL070534

CITATIONS

0

READS

126

7 authors, including:



**Michel Van Camp**

Royal Observatory of Belgium

110 PUBLICATIONS 957 CITATIONS

[SEE PROFILE](#)



**Gwendoline Pajot-Métivier**

Institut national de l'information géographique...

24 PUBLICATIONS 90 CITATIONS

[SEE PROFILE](#)



**Arnaud Watlet**

Université de Mons

17 PUBLICATIONS 10 CITATIONS

[SEE PROFILE](#)



**Alain Dassargues**

University of Liège

217 PUBLICATIONS 2,231 CITATIONS

[SEE PROFILE](#)

Some of the authors of this publication are also working on these related projects:



Earth's free oscillations [View project](#)



URBAN FOOD [View project](#)

All content following this page was uploaded by [Michel Van Camp](#) on 14 September 2016.

The user has requested enhancement of the downloaded file. All in-text references [underlined in blue](#) are added to the original document and are linked to publications on ResearchGate, letting you access and read them immediately.

1 **Direct measurement of evapotranspiration from a forest using a superconducting**  
2 **gravimeter**

3 M. Van Camp<sup>1</sup>, O. de Viron<sup>2</sup>, Gwendoline Pajot-Métivier<sup>3</sup>, Fabien Casenave<sup>3</sup>, Arnaud Watlet<sup>4,1</sup>, Alain Dassargues<sup>5</sup>,  
4 Marnik Vanclooster<sup>6</sup>

5 <sup>1</sup>Royal Observatory of Belgium

6 Seismology-Gravimetry

7 Avenue Circulaire, 3

8 BE-1180 Uccle

9

10 <sup>2</sup>Littoral, Environnement et Sociétés (LIENSs), Université de La Rochelle and CNRS  
11 (UMR7266), France

12

13 <sup>3</sup>IGN LAREG, Univ Paris Diderot, Sorbonne Paris Cité, France

14

15 <sup>4</sup>Université de Mons, Geology and Applied Geology Unit, Belgium

16

17 <sup>5</sup>Université de Liège, Hydrogeology & Environmental Geology, ArGEnCo Dpt, Belgium

18

19 <sup>6</sup>Université catholique de Louvain, Earth and Life Institute, Belgium

20

21

22 Corresponding author: Michel Van Camp (mvc@oma.be)

23

24 **Key Points (140 char):**

25 • Continuous gravity measurements reveal the evapotranspiration of a forested ecosystem  
26 at the mesoscale (~50 ha).

27 • An oak-beech forest evaporates 1.7 mm of water during sunny summer days.

- 28 • Ground gravity is now able to isolate regular signals at the level of a few tenths of mm of  
29 water

30 **Abstract**

31 Evapotranspiration (ET) controls the flux between the land surface and the atmosphere.  
32 Assessing the ET ecosystems remains a key challenge in hydrology. We have found that the ET  
33 water mass loss can be directly inferred from continuous gravity measurements: as water  
34 evaporates and transpires from terrestrial ecosystems, the mass distribution of water decreases,  
35 changing the gravity field.

36 Using continuous superconducting gravity measurements, we were able to identify daily gravity  
37 changes at the level of, or smaller than  $10^{-9}$  nm.s<sup>-2</sup> (or  $10^{-10}$  g) per day. This corresponds to 1.7  
38 mm of water over an area of 50 ha. The strength of this method is its ability to enable a direct,  
39 traceable and continuous monitoring of actual ET for years at the mesoscale with a high  
40 accuracy.

41 **1 Introduction**

42 Improving the assessment of the different components of the terrestrial hydrological  
43 cycle remains a key challenge for geoscientists. A critical component of this cycle is  
44 evapotranspiration (ET), i.e. the process whereby liquid water is converted into water vapor  
45 [Robinson et al., 2003; Sun et al., 2006]. ET encompasses the evaporation flux from soil and  
46 canopy, and the canopy transpiration flux [Monteith, 1965; [Shukla and Mintz, 1981](#)]. The global  
47 ET is more than 85% made up of canopy transpiration, which returns more than 50% of  
48 precipitation back to the atmosphere [[Oki and Kanae, 2006](#)]. In arid to semi-arid environments  
49 ET can return more than 95% of the annual precipitation [Kurc and Small, 2004]; hence its  
50 assessment is critical to assess recharge. ET plays a major role in terrestrial ecosystems. It  
51 controls the amount of green water in the total global water balance and has therefore a major

52 impact on the global fresh water availability [*Rost et al.*, 2008]. Furthermore, ET strongly  
53 controls energy transfer between the Earth and the atmosphere and hence within the global  
54 climate system.

55         The direct accurate and precise measurement of diurnal ET is possible at the individual  
56 plant scale, using weighing lysimeter devices [*Verstraeten et al.*, 2008; *Müller and Bolte*, 2010]  
57 and at the mesoscale, i.e. the scale of a small landscape unit, using eddy-covariance flux towers  
58 [*Shi et al.*, 2008; *Baldocchi and Ryu*, 2011]. Both devices are difficult to implement in  
59 heterogeneous, rugged forested ecosystems. Alternatively, a lysimeter type approach was  
60 proposed to measure ET at the mesoscale [*Barr et al.*, 2000]. Yet, this latter approach relies on  
61 several constraining hypothesis to convert the pressure change obtained by piezometers into ET,  
62 such as e.g. the presence of an aquitard, or a negligible runoff. At the regional scale, ET can only  
63 be estimated indirectly, e.g. from land surface models [*Kelliher et al.*, 1993; *Rana and Katerij*,  
64 2000; *Wilson et al.*, 2001; *Verstraeten et al.*, 2005], and remote sensing still requires terrestrial  
65 measurements for calibration or parametrization [*Jimenez et al.*, 2011]. Such indirect regional  
66 approaches rely also on strong hypotheses, not the least of which is the homogeneity of the  
67 terrain and vegetation attributes in land surface model pixels, inducing a considerable uncertainty  
68 in regional ET assessments [*Baldocchi and Ryu*, 2011; *Hupet et al.*, 2004]. Reducing regional ET  
69 uncertainty therefore relies on the calibration of land surface model parameters, using accurate  
70 and precise real ET data at ground level.

71         We propose a novel way to measure the mesoscale (about 50 ha) ET continuously, based  
72 on continuous gravity monitoring. Gravity is the acceleration experienced by a body at rest at the  
73 Earth surface, due to the combined gravitational forces of the Earth, the Moon, the Sun, and the  
74 planets, and the centrifugal effect from the Earth rotation. Continuous gravity monitoring using

75 up-to-date instruments is precise to 1 part per 100 billion ( $10^{-11}$  g) [Van Camp et al., 2006].  
76 Further, celestial mechanics can provide the relative positions of the Earth, the Moon, and the  
77 Sun. The contribution from these bodies can be corrected into the gravity data down to a  
78 resolution of at least  $10^{-11}$  g [Hartmann and Wenzel, 1995; Wenzel, 1996], so that only the signal  
79 from the Earth system is left in the gravity data. The Earth rotation is also monitored with high  
80 accuracy, which allows a precise correction for the time variation of the centrifugal effect. The  
81 atmospheric contribution can be estimated and corrected with precise meteorological data such  
82 as the surface pressure. Traditional hydrology-gravity studies remove all these effects to study  
83 changes in terrestrial water content, the dominant signal in the corrected gravity time-series  
84 coming from the mesoscale terrestrial water content directly around the instrument [Creutzfeldt  
85 et al., 2008] (Figure S1). We go one step further and remove the gravity effect of interflow losses  
86 to evaluate losses caused by ET during periods without rainfall, showing that gravity time series  
87 can be used as a weighing lysimeter for measuring mesoscale ET over a rain-free period.

## 88 **2 Continuous gravity measurements**

89 In 1995, a superconducting (or cryogenic) gravimeter (SG) [Goodkind, 1999] was  
90 installed in the Membach station, eastern Belgium (50.6°N, 6.0°E, altitude: 250 m), and has been  
91 continuously operating ever since. Basic processing of the SG data is done as described by  
92 Hinderer et al. [2007]. The instrumental drift of the SG is corrected using repeated absolute  
93 gravity measurements. In this study, tides were removed by computing tidal parameter sets using  
94 the ETERNA package [Wenzel, 1996] on the gravity time series extending from 2004-06-01 to  
95 2015-01-03 (3825.75 record days). The tidal potential is the Hartmann-Wenzel [Hartmann and  
96 Wenzel, 1995] catalog with 7761 waves. The adjusted tidal parameters make it possible to  
97 compute a tidal signal which includes both the solid Earth tide and ocean loading effects. The

98 atmospheric loading effects were corrected by using a linear admittance factor also provided in  
99 the ETERNA package. It amounts to  $-3.302 \text{ nm}\cdot\text{s}^{-2} \text{ hPa}^{-1}$ . An annual modulation effect on the  
100 atmospheric S3 tide remained after removing the tidal and atmospheric effects. It was removed  
101 by fitting two harmonics with frequencies of (3 cpd + 1 cpy) and (3 cpd - 1 cpy) on the gravity  
102 residuals [Polzer et al., 1996].

### 103 **3 Soil moisture**

104 The station is located about fifty meters below the surface (Figure S2). The area is one of  
105 deciduous forest (Figure S3) and experiences a marine temperate climate (Cfb in the climate  
106 scheme of Köppen–Geiger [Peel et al., 2007]) (Figure S4). Given the position of the nearby  
107 river, the low saturated hydraulic conductivity and the low porosity of the bedrock in which the  
108 station is excavated [Van Camp et al., 2006], the diurnal signal coming from nearby aquifers or  
109 river is expected to be smaller than  $0.1 \text{ nm/s}^2$ , i.e. much smaller than the ET signature.

110 Since 2004, three soil moisture time domain reflectometry (TDR) probes at 30, 45 and 60  
111 cm below the surface allow for a continuous monitoring of the gravimetric water content (GWC,  
112 the mass of water per unit mass of dry soil) in the partially saturated soil, 48 m above the SG  
113 [Van Camp et al., 2006]. The corresponding time series, which measures the local-scale water  
114 saturation of the soil, shows a seasonal pattern with steps during rainfall events [Van Camp et al.,  
115 2006; Meurers et al., 2007]. Focusing on a dry period, of which a short sample is plotted in red  
116 on Figure S5, we observe that the soil moisture decreases only during the day. This signature is  
117 expected from evapotranspiration during dry days [Schelde et al., 2011].

118 A small soil moisture increase is seen overnight, probably due to hydraulic lift effects  
119 [Caldwell et al., 1998], vapor condensation, capillary water redistribution, or imperfect  
120 temperature correction of the probes. The soil moisture probes only allow the first 60 cm of the

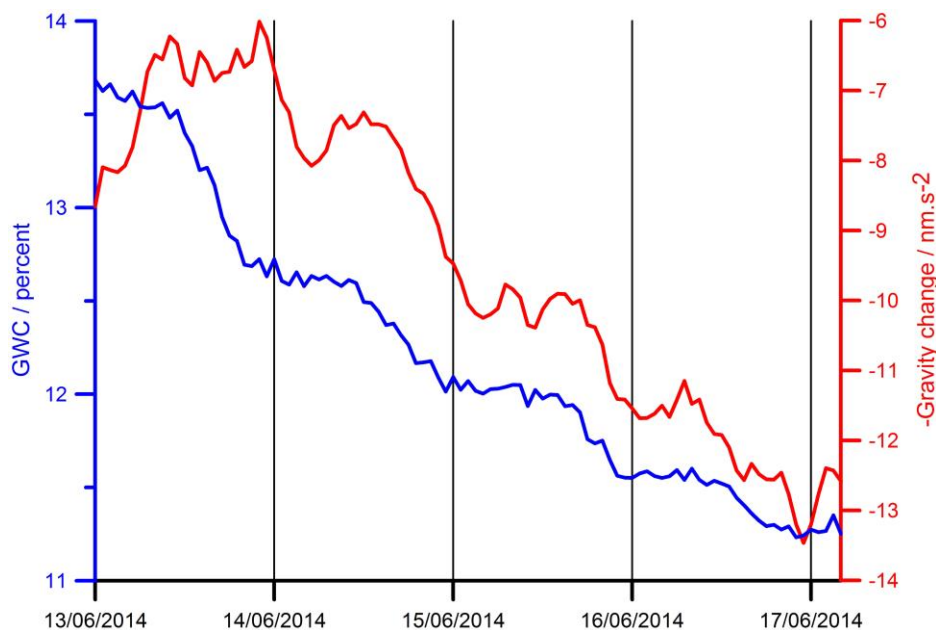


121 soil to be investigated. For this reason we want to study the potential of gravity measurements to  
 122 assess ET at the mesoscale around the station.

#### 123 **4 Modeling the gravity effect of groundwater**

124 Measuring the gravity signature of ET is a metrological challenge, as the expected signal  
 125 is at the level of a few millimeters of water in a temperate deciduous forest [*Kosugi et al., 2006*].  
 126 For the diurnal cycle, the geophysical noise, mostly caused by hydrogeological effects and  
 127 imperfect correction of atmospheric factors, amounts to  $0.4 \text{ nm.s}^{-2}$ , corresponding to 1.0 mm of  
 128 water. Hence the expected ET signal is at the limit of the precision level of terrestrial  
 129 measurements [*Van Camp et al., 2005*], and can only be evidenced at particularly favorable  
 130 times (Figure 1A). To enhance the signal in the time series, a stacking process over at least a few  
 131 dozen of days was needed to isolate the signal (Figures 1B and 1C).

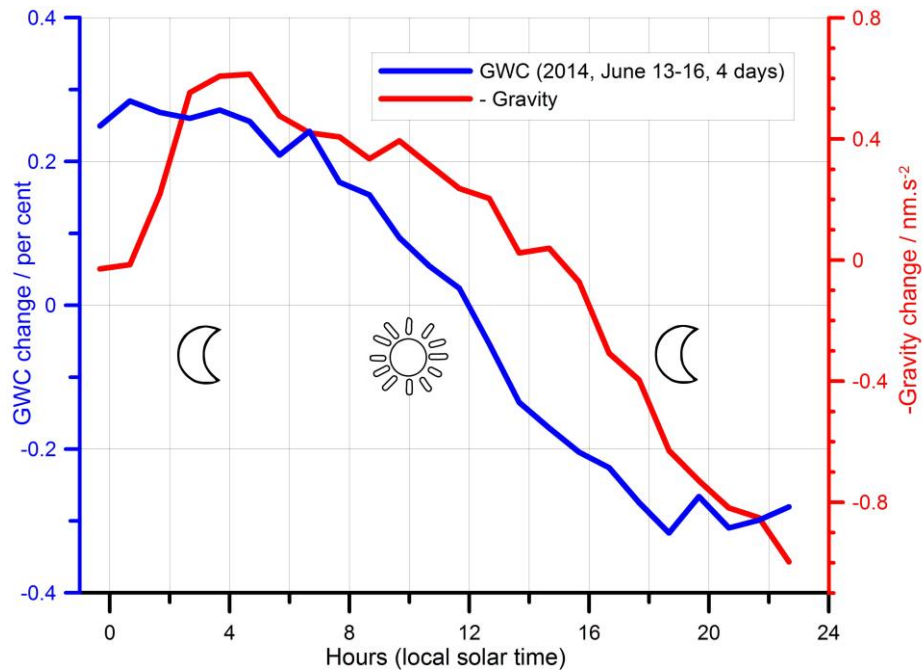
132



133

134

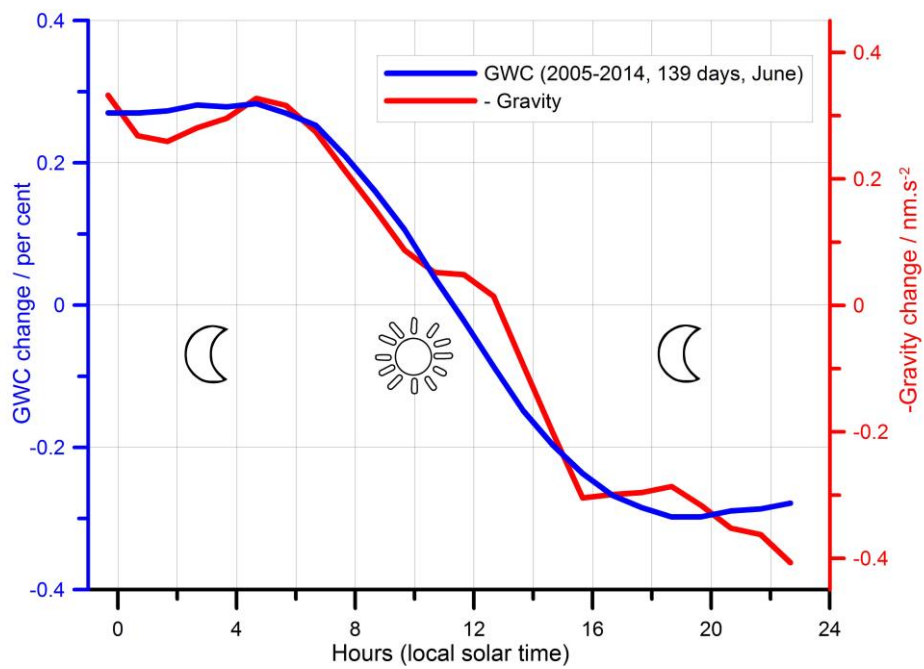
(A)



135

136

(B)



137

138

(C)

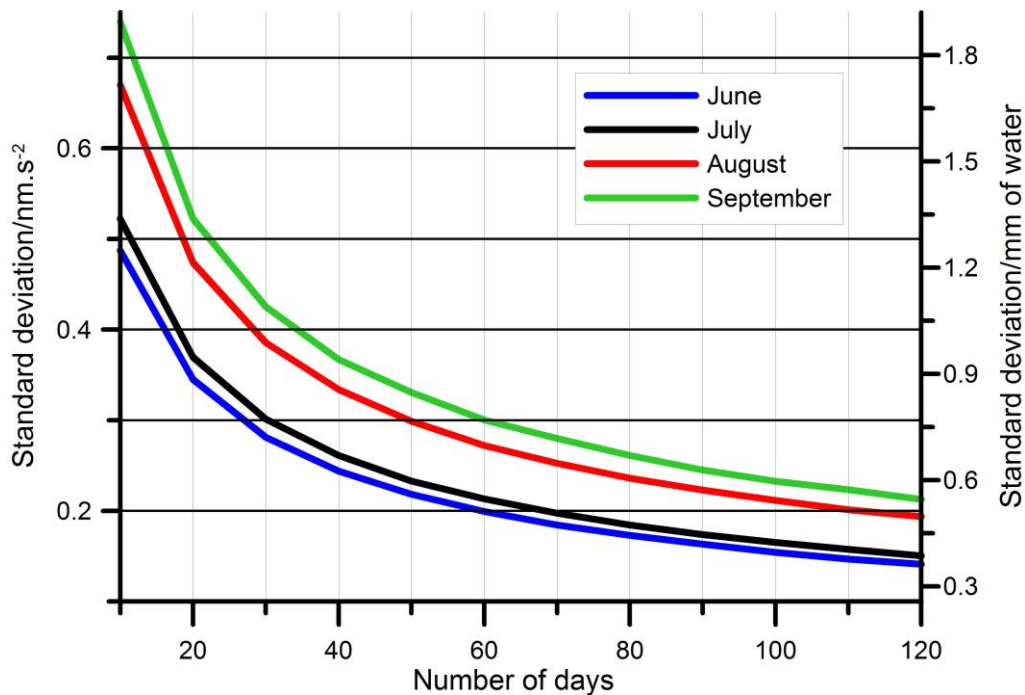
139

140

**Figure 1.** Gravity water content (blue, in %) and inverted gravity signal (red, in  $\text{nm.s}^{-2}$ ); the actual gravity signal increases because the gravimeter is underground, below the

141 surface soil moisture). Time is in days (A) and hours (B, C, local solar time). (A) Series  
142 during 4 days in June 2014. An decrease in gravity of about  $2 \text{ nm.s}^{-2}$ , equivalent to a loss  
143 of 5 mm of water, is observed during the day; (B) stacked values as shown on (A); (C)  
144 stacked values for 139 dry days. The stacking is performed in the months of June from  
145 2005 to 2014. Between 4:40 and 17:40 the GWC diminishes by  $-0.57 \pm 0.02$  percentage  
146 point and gravity increases by  $0.66 \pm 0.14 \text{ nm/s}^2$ , which is equivalent to  $1.7 \pm 0.3$  mm of  
147 water. The subsurface lateral flow was separated from the diurnal ET signal by removing  
148 a linear trend fitted over the nighttime pattern.

149 Figure 2 shows the error on the gravity signal calculated as a function of the number of  
150 days. This is done for June, July, August and September, during which more than 120 data  
151 values are available. The errors were estimated by the Monte-Carlo method using 100,000  
152 random resamples [Robert and Casella, 2004]. A precision of  $0.2 \text{ nm.s}^{-2}$ , equivalent to 0.5 mm  
153 of water, is already obtained after 60 days in June and 70 days in July, while 120 days or more  
154 are necessary for August and September, as ET decreases when summer fades to fall (Figure S6).



155

156 **Figure 2.** The standard deviation of the daily gravity changes as a function of the number  
 157 of days. This provides the number of days necessary to measure the daily gravity change,  
 158 for the 4 months of which more than 120 data are available. A precision of 0.2 nm/s<sup>2</sup>,  
 159 equivalent to 0.5 mm of water, is obtained when 60 days or are available in June and 70  
 160 in July.

161 From 2005 to 2014, we selected dry periods, i.e. periods when the soil moisture data  
 162 exhibits step-like behavior as on Figure S5. This resulted in 139 days in June, i.e. the month  
 163 experiencing the strongest ET effect (Figure S6). We averaged the gravity values separately for  
 164 each hour of the day, to obtain an averaged diurnal cycle. The averaged cycle is illustrated for  
 165 both the soil moisture and the gravity in Figures 1B and 1C. On Figure 1C, the stair-like  
 166 behavior is clear in the stacked soil moisture data, as well as the small increase during the night.  
 167 The stair-like behavior in the gravity data is also present. From July to September, the signal  
 168 decreases and falls within the error bars, making it difficult to extract.

169 Note that the TDR probes and the gravimeter do not perform the same kind of  
170 measurement, otherwise there would be no challenge in obtaining the ET, and it would long be  
171 public knowledge. At the Membach station, the TDR probes clearly show fast changes in the  
172 shallowest zone above 60 cm. Given the hydrogeological context in the weathered zone,  
173 drainage is quite efficient and TDRs cannot reflect the water dynamics in the whole unsaturated  
174 weathered zone (1-10 m thick [*Van Camp et al.*, 2006]), nor in neighboring zones. We only use  
175 the GWC as a measurement of the saturation conditions of the first 60 centimeters, allowing us  
176 to identify dry periods. In the gravity signal, there is a residual slope, visible during the night,  
177 caused by the subsurface lateral flow. This flow was separated from the diurnal ET signal by  
178 removing a linear trend fitted over the nighttime behavior. This flow is caused by an ongoing  
179 interflow (subsurface lateral flow) process at the base of the weathered zone lower than the soil  
180 moisture probes [*Kosugi et al.*, 2006; *Davies-Smith et al.*, 1988]. This interflow occurs in lower  
181 layers of the ground and is consequently not observed by the TDR probes, except just after  
182 strong rainfalls.

183 From those average days, we estimate the daily gravity increase associated to the ET at the  
184 level of  $0.66 \pm 0.14$  nm/s<sup>2</sup>. Note that gravity increases because the gravimeter is located  
185 underground, below the surface soil moisture. This corresponds to an average of  $1.7 \pm 0.3$  mm of  
186 water over the area. Details on the conversion of nm/s<sup>2</sup> to mm of water are available in the  
187 supporting information [*Okabe*, 1979].

188 This value compares with what is expected in such a Cfb humid, temperate climate  
189 [*Baldocchi et al.*, 2011], and with the  $1.9 \pm 0.2$  mm estimate from an eddy covariance tower in a  
190 similar forest in Vielsalm (50.3°N, 6.0°E, altitude: 450 m), 34 km south of Membach [*Soubie*,  
191 2014]. Comparing Membach and Vielsalm is only indicative, given that (1) the techniques are

192 different, (2) ET depends on the stand (Douglas fir and beeches in Vielsalm [Aubinet et al.,  
193 2001]), topography, altitude, soil conditions, canopy density, age and forest management, (3) ET  
194 inferred from the flux tower includes rainy days.

195         This also compares with the potential ET (PET) of 3.9 mm estimated by using the  
196 Penman–Monteith equation, considering PET as the maximum ET (see supporting information,  
197 equation [Allen et al., 1998; Verstraeten et al., 2005]. PET is the amount of evaporation that  
198 would occur if sufficient water was available. The PET and the ET inferred from the gravity  
199 changes are computed on the same dry days. This differs from the eddy covariance estimates,  
200 which are computed taking all the days of the month into account.

201 **5 Discussions**

202 In the subsurface, evapotranspiration is a major hydrological phenomenon that occurs in dry  
203 days, which is well illustrated by the GWC data at the Membach station. Considering that this  
204 phenomenon must be linked to changes in the water distribution around the gravimeter, it is  
205 theoretically possible to retrieve the associated signature in the gravity signal. Several questions,  
206 however, remain concerning those results:

207 First, are those results robust and reproducible elsewhere? We successfully tested the robustness  
208 for the Membach station in many ways by taking different years and different times of the year.  
209 It is not possible to infer from the available data if the same can be achieved in other stations. We  
210 applied our method to one other station, Walferdange, in Luxembourg, and we obtained similar  
211 results. However, based on this single comparison, we cannot conclude that the method would  
212 work at every site. Considering the level of the signal, reproducing these results in another  
213 station will require working closely with the operator of the station.

214 Also, can we be sure that the obtained signature is indeed linked to evapotranspiration?  
215 Considering that (1) the amplitude is of the right order of magnitude, (2) the signal cannot be  
216 retrieved at winter time when ET is reduced, (3) the signal disappears when it is raining, (4) as  
217 soon as we avoid rainy days, the diurnal gravity signal shows this signature that only exists  
218 during the day, we can have some confidence in the results.

219 Finally, what is the scope of this study if it only applies to one or two stations? We consider that,  
220 even in this case, this study is useful for three reasons:

221 (1) From the measurement point of view, it is interesting to show that an appropriate correction  
222 of the data enables a signal to be retrieved down to a resolution of a few tenths of  $\text{nm/s}^2$ ;

223 (2) This study provides for the first time a direct measurement of evapotranspiration integrated  
224 over a deciduous forest area, a result interesting in its own right;

225 (3) New methods to estimate evapotranspiration can be validated and calibrated on a site where  
226 SG gravity provides an independent estimate. Note that Membach is probably not an ideal case  
227 given that the topography and the geology of the subsurface (i.e. silty soil combined with  
228 sandstone blocks and gravels) are likely to cause a strong subsurface lateral flow which is likely  
229 to disrupt the signal. We think that the ideal site would be in a flat forested area (if possible,  
230 installing the gravimeter in a shaft), with lower underground hydraulic conductivity.

## 231 **6 Conclusions**

232 We have shown that liquid water losses can be directly inferred from continuous gravity  
233 measurements: as water evaporates and transpires from terrestrial ecosystems, the mass  
234 distribution varies through the system, changing its gravity field.

235 Using continuous superconducting gravity measurements, we were able to identify  
236 average daily changes in gravity at the level of, or smaller than  $10^{-9} \text{ nm.s}^{-2}$  (or  $10^{-10} \text{ g}$ ) per day.  
237 Considering the topography around the gravimeter, this corresponds in June, from 2005 to 2014,  
238 to an average of 1.7 mm of water per sunny day over an area of 50 ha. The strength of this  
239 method consists in its ability to ensure a direct, traceable and continuous monitoring of actual ET  
240 for years at the mesoscale ( $\sim 50 \text{ ha}$ ) with a precision of a few tenths of mm of water.

241 This can be performed in rugged forested areas with a precision of a few tenths of mm of  
242 water. The method is, therefore, complementary to the well-known eddy covariance method



243 which often suffers from methodological uncertainty due to poor footprint modeling. This study  
244 provides also a way to assess the quality of the gravity time series and the applied corrections.

## 245 **Acknowledgments and Data**

246 We thank B. Meurers (U. Vienna) and W. Zürn (BFO) for their advice about the correction of the  
247 tidal effects and M. Vandiepenbeeck (RMI) for providing the weather time series. S. Castelein,  
248 M. Hendrickx, G. Rapagnani, P. Bizermana, R. De Dobbeleer, M. De Knijf, B. Frederick and V.  
249 Rogge provided invaluable help for the maintenance of the Membach station. We thank the  
250 forester A. Delclissar for allowing us to perform hydrological measurements in the forest. We are  
251 grateful to O. Francis (U. Luxembourg) for the Walferdange data and ongoing fruitful  
252 discussions. We thank two anonymous reviewers and the Editor Valeriy Ivanov for their valuable  
253 reviews. Work from OdV was financially supported by CNES through the TOSCA program and  
254 the Institut Universitaire de France. Data are available for academic purposes through the  
255 website of the Royal Observatory of Belgium:  
256 <http://seismo.oma.be/en/gravimetry/observations/online-database>.

## 257 **References**

- 258 Allen, R.G., L.S. Pereira, D. Raes, and M. Smith (1998), FAO Irrigation and drainage paper No.  
259 56., *Rome Food Agric. Organ. U. N.*, 26–40.
- 260 Aubinet, M., et al. (2001), Long term carbon dioxide exchange above a mixed forest in the  
261 Belgian Ardennes, *Agric. For. Meteorol.* 108, 293-315, doi:10.1016/S0168-  
262 1923(01)00244-1.
- 263 Baldocchi, D. D., and Y. Ryu (2011), A Synthesis of Forest Evaporation Fluxes –from Days to  
264 Years – as Measured with Eddy Covariance, in *Forest Hydrology and Biogeochemistry:*

- 265           Synthesis of Past Research and Future Directions, edited by D. F. Del Lavia, D. E.  
266           Carlyle-Moses and T. Tanaka, vol. 216 of Springer series in Ecological Studies, pp. 101-  
267           116, doi:10.1007/978-94-007-1363-5\_5.
- 268 [Barr, A.G., G. van der Kamp, R. Schmidt, and T. Andrew Black \(2000\), Monitoring the moisture](#)  
269           [balance of a boreal aspen forest using a deep groundwater piezometer. \*Agric. For.\*](#)  
270           [Meteorol., 102, 13-24, doi:10.1016/S0168-1923\(00\)00094-0.](#)
- 271 Creutzfeldt, B., A. Güntner, T. Klügel, and H. Wziontek (2008), Simulating the influence of  
272           water storage changes on the superconducting gravimeter of the Geodetic Observatory  
273           Wetzell, Germany, *Geophysics*, 73(6), doi:10.1190/1.2992508.
- 274 Caldwell, M. M., T. E. Dawson, and J. H. Richards (1998), Hydraulic Lift: Consequences of  
275           Water Efflux from the Roots of Plants, *Oecologia*, 113, 151-161.
- 276 [Davies-Smith, A., E. L. Bolke, and C. A. Collins \(1988\), Geohydrology and digital simulation of](#)  
277           [the ground-water flow system in the Umatilla Plateau and Horse Heaven Hills area,](#)  
278           [Oregon and Washington, U.S. Geol. Survey Water-Resources Inv. Rep. 87-4268.](#)
- 279 [Goodkind, J . M. \(1999\), The superconducting gravimeter, \*Rev. Sci. Instrum.\*, 70, 4131– 4152,](#)  
280           [doi:10.1063/1.1150092.](#)
- 281 [Hartmann, T., and H.-G. Wenzel \(1995\), The HW95 tidal potential catalogue, \*Geophys. Res.\*](#)  
282           [Lett., 22, 3553-3556, doi:10.1029/95GL03324.](#)
- 283 Hinderer, J., D. Crossley, and R. J. Warburton (2007), Gravimetric Methods – Superconducting  
284           Gravity Meters, *Treatise on Geophysics*, edited by T. Herring and G. Schubert, vol. 3, pp.  
285           65–122, doi:10.1016/B978-044452748-6/00172-3.

- 286 Hupet, F., P., Bogaert, and M. Vanclooster (2004), Quantifying the local scale uncertainty of  
287 estimated actual evapotranspiration, *Hydrol. Process.* **18**, 3415-3434,  
288 doi:10.1002/hyp.1504.
- 289 Jiménez, C., et al. (2011), Global intercomparison of 12 land surface heat flux estimates, *J.*  
290 *Geophys. Res.*, 116, D02102, doi:10.1029/2010JD014545.
- 291 Kelliher, F. M., R. Leuning, and E.-D. Schulze(1993), Evaporation and canopy characteristics of  
292 coniferous forests and grasslands, *Oecologia* , **95**, 153-163.
- 293 Kosugi, K., S. Katsura, M. Katsuyama, and T. Mizuyama (2006), Water flow processes in  
294 weathered granitic bedrock and their effects on runoff generation in a small headwater  
295 catchment, *Water Resour. Res.*, **42**, W02414, doi:10.1029/2005WR004275.
- 296 Kurc, S. A., and E. E. Small (2004), Dynamics of evapotranspiration in semiarid grassland and  
297 shrubland ecosystems during the summer monsoon season, central New Mexico, *Water*  
298 *Resour. Res.*, **40**, W09305, doi:10.1029/2004WR003068
- 299 Meurers, B., M. Van Camp, and T. Petermans (2007), Correcting gravity time series using  
300 rainfall modeling at the Vienna and Membach stations and application to Earth tide  
301 analysis. *J. Geod.*, **81**, 703-712, doi:10.1007/s00190-007-0137-1.
- 302 Monteith, J. L. (1965), Evaporation and environment, *Symp. Soc. Expl. Biol.*, **19**, 205-234.
- 303 Müller, J., and A. Bolte (2010), Forest hydrology research with lysimeter in the northeast  
304 German lowlands special methods and results for the forest management, in *Soil*  
305 *solutions for a changing world : proceedings of the 19th World Congress of Soil Science*,  
306 edited by R. J. Gilkes and N. Prakongkep, pp 28-31.

- 307 Okabe, M. (1979), Analytical expressions for gravity anomalies due to homogeneous polyhedral  
308 bodies and translations into magnetic anomalies, *Geophysics*, *44*, 730-741,  
309 doi:10.1190/1.1440973.
- 310 Okai, T., and S. Kanae (2006), Global Hydrological Cycles and World Water Resources, *Science*,  
311 *313*, 1068-1072, doi:10.1126/science.1128845.
- 312 Peel, M. C., B.L. Finlayson, and T .A. McMahon (2007), Updated world map of the Köppen–  
313 Geiger climate classification, *Hydrol. Earth Syst. Sci. Discuss.*, *11*, 1633–1644,  
314 doi:10.5194/hess-11-1633-2007.
- 315 G. Polzer, W. Zürn, and H.-G. Wenzel (1996), NDFW Analysis of Gravity, Strain, and Tilt Data  
316 from BFO, *Bull. Inf. Marées Terrestres*, *125*, 9514 – 9545.
- 317 Rana, G., and N. Katerji (2000), Measurement and estimation of actual evapotranspiration in the  
318 field under Mediterranean climate: A review, *Eur. J. Agron.*, *13*, 125–153,  
319 doi:10.1016/S1161-0301(00)00070-8.
- 320 Robert, C., and G. Casella (2004), Monte Carlo Statistical Methods; Springer, New-York,  
321 doi:10.1007/978-1-4757-4145-2
- 322 Robinson, M., et al. (2003), Studies of the impact of forests on peak flows and baseflows: a  
323 European perspective, *For. Ecol. Manage.*, *186*, 85-97, doi:10.1016/S0378-  
324 1127(03)00238-X.
- 325 Rost, S., D. Gerten, A. Bondeau, W. Lucht, J. Rohwer, and S. Schaphoff (2008), Agricultural  
326 green and blue water consumption and its influence on the global water system, *Water*  
327 *Resour. Res.*, *44*, W09405, doi:10.1029/2007WR00633

- 328 Schelde, K., et al. (2011), Comparing Evapotranspiration Rates Estimated from Atmospheric  
329 Flux and TDR Soil Moisture Measurements, *Vadose Zone J.*, *10*, 78–83,  
330 doi:10.2136/vzj2010.0060.
- 331 [Shi, T.-T., D.-X. Guan, J.-B. Wu, A.-Z. Wang, C.-J. Jin, and S.-J. Han \(2008\), Comparison of](#)  
332 [methods for estimating evapotranspiration rate of dry forest canopy: Eddy covariance,](#)  
333 [Bowen ratio energy balance, and Penman-Monteith equation, \*J. Geophys. Res.\*, \*113\*,](#)  
334 [D19116, doi:10.1029/2008JD010174.](#)
- 335 Soubie, R. Evaluation de l'évapotranspiration réelle, de ses composantes et de sa régulation dans  
336 un peuplement composé de hêtres et de douglas : analyse comparative de l'effet espèce et  
337 des méthodes d'évaluation, *thesis*, Université Catholique de Louvain (2014).
- 338 [Shukla, J., and Y. Mintz \(1981\), Influence of Land-Surface Evapotranspiration on the Earth's](#)  
339 [Climate, \*Science\*, \*215\*, 1498-1501, doi:10.1126/science.215.4539.1498.](#)
- 340 Sun, G., G. Zhou, Z. Zhangc, X. Wei, S. G. McNulty, and J. M. Vose (2006), Potential Water  
341 Yield Reduction due to Reforestation Across China, *J. Hydrol.*, *328*, 548-558,  
342 doi:10.1016/j.jhydrol.2005.12.013.
- 343 [Van Camp, M., S. D. P. Williams, and O. Francis \(2005\), Uncertainty of absolute gravity](#)  
344 [measurements, \*J. Geophys. Res.\*, \*110\*, B05406, doi:10.1029/2004JB003497.](#)
- 345 Van Camp, M., M. Vanclooster, O. Crommen, T. Petermans, K. Verbeeck, B. Meurers, T. van  
346 Dam, and A. Dassargues (2006a), Hydrogeological investigations at the Membach  
347 station, Belgium, and application to correct long periodic gravity variations, *J. Geophys.*  
348 *Res.*, *111*, B10403, doi:10.1029/2006JB004405.

- 349 Verstraeten, W. W., B. Muys, J. Feyen, F. Veroustraete, M. Minnaert, L. Meiresonne, and A. de  
350 Schrijver (2005), Comparative analysis of the actual evapotranspiration of Flemish forest  
351 and cropland, using the soil water balance model WAVE, *Hydrol. Earth Syst. Sci.*, *9*,  
352 225–241, doi:10.5194/hess-9-225-2005.
- 353 Verstraeten, W. W., F. Veroustraete, and J. Feyen (2008), Assessment of evapotranspiration and  
354 soil moisture content across different scales of observation, *Sensors*, *8*, 70–117,  
355 doi:10.3390/s8010070.
- 356 Wenzel, H.-G. (1996), The nanogal software: Earth tide data processing package ETERNA 3.30,  
357 *Bull. Inf. Marées Terrestres*, *124*, 9425–9439 .
- 358 Wilson, K.B., P. J. Hanson, P. J. Mulholland, D. D. Baldocchi, and S. D. Wullschleger (2001), A  
359 comparison of methods for determining forest evapotranspiration and its components:  
360 Sap-flow, soil water budget, eddy covariance and catchment water balance. *Agric. For.*  
361 *Meteorol.*, *106*, 153–168, doi:10.1016/S0168-1923(00)00199-4.